Semiconductors, 2022, Vol. 56, No. 9

Calcium fluoride films with $2-10$ nm thickness on Silicon-(111): growth, diagnostics, study of the through current transport

© *A.G. Banshchikov, M.I. Vexler, I.A. Ivanov, Yu.Yu. Illarionov, N.S. Sokolov, S.M. Suturin*

Ioffe Institute,
194021 St. Petersburg, Russia

E-mail: vexler@mail.ioffe.ru

Received May 12, 2022
Revised June 30, 2022
Accepted June 30, 2022

Epitaxial calcium fluoride (CaF_2) layers with a nominal thickness up to 10 nm on the (111)-oriented Silicon (Si) are obtained. Surface topographies of the fluoride films are recorded and the current-voltage characteristics of the Au/CaF_2/Si structures are studied. On a qualitative level, these structures exhibited all the features usual for metal-insulator-semiconductor systems. The current-voltage curves of the samples were reproduced by modeling considering a finite ($0.1-1$ nm) value of the standard thickness deviation of the dielectric CaF_2 film.

Keywords: calcium fluoride, thin films, MIS structure, leakage current.

DOI: 10.21883/SC.2022.09.54133.9885

1. Introduction

Thin epitaxial fluoride (specifically, calcium fluoride CaF_2) layers have been studied for over 30 years [1–4], although these studies were understandably less extensive than the examination of silica SiO_2 and other traditional oxide insulators [5]. The interest in calcium fluoride stems from the fact that some of its „dielectric parameters“ are better than those of SiO_2; specifically, its permittivity is $\varepsilon = 8.43$ (the corresponding value for SiO_2 is 3.9), its band gap is $E_g = 12.1$ eV (8.9 eV), and the effective electron mass in CaF_2 is $m_e = 1.0m_0$ ($0.42m_0$) [6].

The similarity between the lattice constants of CaF_2 and silicon provides an opportunity to grow layers of one material on the surface of the other and thus produce high-quality metal–insulator–semiconductor (MIS) structures. For thermodynamic reasons, epitaxial growth of CaF_2 is feasible only on Si(111) substrates.

Fluoride films with a thickness of $1-2$ nm may be used as barrier layers in resonant tunneling diodes and superlattices [7] (in both cases, in combination with CdF_2 or Si); they are also regarded as competitive to high-k dielectrics for field-effect transistors of traditional designs (and not only on silicon [8]).

It has been established relatively recently that the application of CaF_2 instead of SiO_2, Al_2O_3, or hBN allows one to improve the characteristics of transistors with two-dimensional channels fabricated from, e.g., MoS_2 [9,10]. Compared to usual field-effect transistors, such transistors (see, e.g., [9–12]) allow one to „progress“ further in the direction of miniaturization. Molybdenum disulfide in these structures is deposited on top of an epitaxial fluoride film. Slightly thicker (on the order of 10 nm) fluoride layers are more suitable for such devices than ultrathin films with a thickness of $1-2$ nm. Therefore, the issue of growth and testing of CaF_2 films of the corresponding thickness range becomes topical.

It is known from previous experience that fluoride films with a thickness of $5-20$ nm are harder to fabricate than $2-3$-nm-thick films. However, even if the quality of thicker layers is somewhat lower, their dielectric properties still need to be examined, at least for general insight. With the role played by a dielectric in CaF_2/MoS_2 transistors taken into account, the problem of measurement of the through current enters into in the foreground of experimental research. It is also important to examine the stability of characteristics, which needs to be known in order to estimate the performance efficiency of electronic devices.

We first present the key aspects of fluoride growth technology, details of the experiment, and examples of the recorded CaF_2 surface relief. Current–voltage (I–V) curves of MIS structures with such layers and the results of their reproduction in modeling are reported next. Conclusions regarding the quality of the obtained films are made at the end of the paper.

2. Samples and experimental procedure

MIS structures with a calcium fluoride layer grown by molecular beam epitaxy (MBE) on a substrate of moderately doped *n*-Si (the donor density was $\sim 10^{17}\,\mathrm{cm}^{-3}$) were examined. Nominal thickness d_n of the CaF_2 film was $2-10$ nm.

While a certain number of studies focused on films with a thickness of ~ 2 nm have already been published, we are essentially the first to make an attempt at growing $5-10$-nm-thick fluorides.

The MBE process was specific in that a low (250°C) growth temperature was chosen. This choice helped avoid the formation of triangular pinholes [13] that are typical of

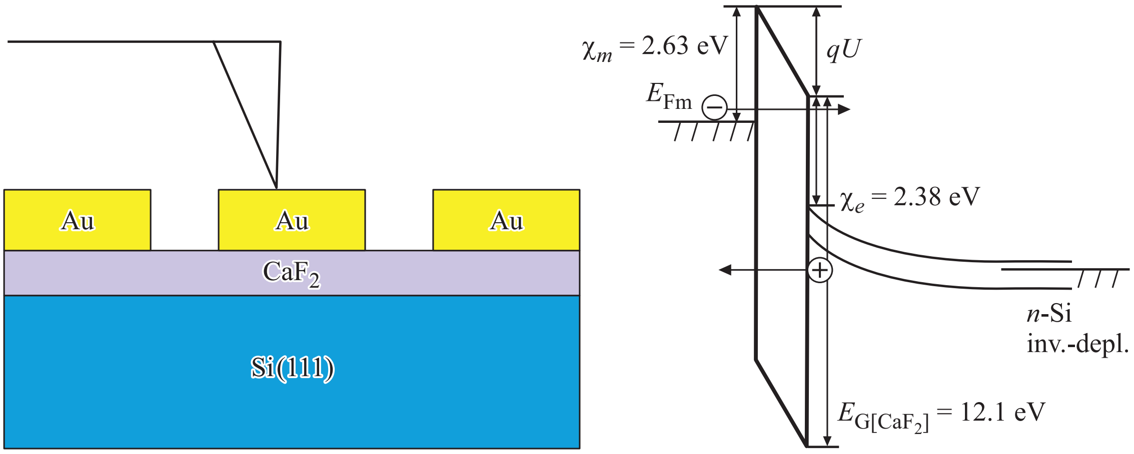

Figure 1. Schematic diagram of a substrate with deposited electrodes and a cantilever contacting to one of them. Band diagram of the Au/CaF_2/Si system (reverse bias).

films obtained at a temperature of $\sim 600^\circ$C and reduce the resistance to unacceptable levels.

The rms CaF_2 surface roughness was measured with an atomic force microscope (AFM).

Circular gold electrodes with a diameter of $70\,\mu$m and a thickness of $\sim 0.1\,\mu$m were deposited on top of a fluoride layer through a mask. An Au/CaF_2/n-Si(111) structure was produced as a result. An array of 500–1000 structures was fabricated in one wafer (Fig. 1).

Steady-state I–V curves were measured. The AFM cantilever with gold coating was used to apply voltage to the top electrode. The substrate was grounded on the back side.

I–V curves were recorded within the range of $-2\ldots+2$ V with a Keithley-2400 source meter controlled by home-made software. Measurements were performed at room temperature in the dark and under illumination (the presence of irradiation is hereinafter explicitly stated).

3. Fluoride surface topography

The surface topography of the grown CaF_2 layer was imaged by AFM. These images helped, first, estimate the state of the surface as a whole and, second, determine the rms roughness.

Several types of irregularities were identified. First, „needles“ of a small planar size and a height up to 20 nm were observed. Second, contamination of the grown film was evident in certain cases. Third, common nanometer-scale irregularities attributable to random causes were present.

Presumably, the emergence of pointy needles is attributable to the local formation of silicon carbide SiC islets; naturally, such defects distort the CaF_2 relief within a certain region. The cases with a significant number of such needles or post-growth contamination were treated as irrelevant and were excluded from consideration. Figure 2 presents an image without such defects.

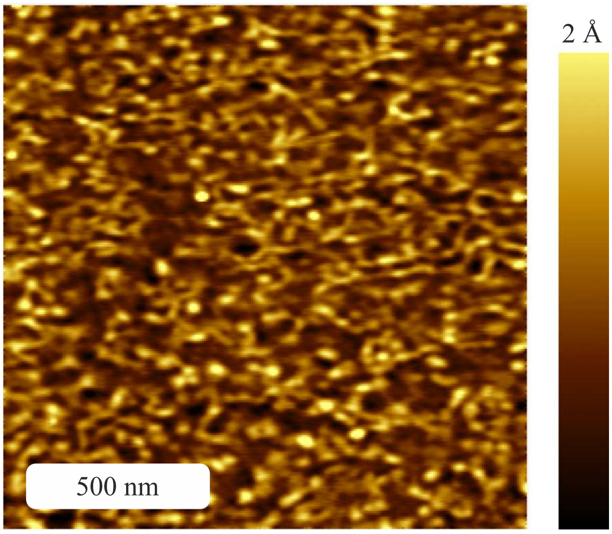

Figure 2. AFM image of the surface of the grown CaF_2 film with a thickness of ~ 5 nm.

The rms roughness for selected samples varied from several angstroms (0.1–0.2 nm) to a nanometer (~ 1.0 nm). This is essentially the standard deviation of thickness σ_d, since the initial Si substrate surface was atomically smooth. A general trend toward an increase in rms roughness with nominal thickness d_n was noted. This is hardly surprising: if the standard deviation of thickness d_{ml} of a single monolayer is σ_{ml}, the deviation for N monolayers (i.e., for nominal thickness $N \times d_{\text{ml}}$) is mathematically not lower than $N^{1/2}\sigma_{\text{ml}}$. The rms roughness of the thinnest layers, which were fabricated mostly for the sake of completeness (5–10-nm-thick layers are more interesting for a number of reasons), was approximately the same as the one of the best films with $d_n \sim 2\,\text{nm}$ examined in our earlier studies [14].

4. On the calculation of I–V-characteristics

The calculation of I–V curves of tunnel MIS structures with their thickness d being uniform throughout the area is no novelty and is relatively easy to perform [15].

The following aspects of our calculation deserve a mention. We took into account the presence of two current components (metal–Si conduction band and metal–Si valence band), the quantization of states near the Si/insulator interface, and the conservation of the transverse component of the wave vector [14]. The last factor is significant in the context of transport specifically through crystalline insulators, of which CaF_2 is an example.

The height of the barrier between the metal and the conduction band edge of calcium fluoride was taken equal to 2.63 eV, and the CaF_2/Si conduction band discontinuity was set to $\chi_e = 2.38\,\text{eV}$ (Fig. 1).

Calculations were performed under the standard assumption of equilibrium in the substrate (i.e., the presence of a single Fermi level for electrons and holes was assumed). It will be shown below that this assumption actually holds true even for the thinnest examined fluoride films (hypothetically, owing to the deficiency of minority carriers, the current under reverse polarity in them may exhibit plateau instead of increasing with voltage [16]).

The fluoride thickness nonuniformity was taken into account through integration: $\langle j \rangle = \int j(d) f(d, d_n, \sigma_d)\delta d$, where $f(d, d_n, \sigma_d)$ is the Gaussian density.

It is instructive to consider the nature and scale of calculated variations for a given nominal d_n and adjusted parameter σ_d (Fig. 3) prior to examining the experimental data. The value of $d_n = 5\,\text{nm}$ was chosen for definiteness; it can be seen that the current rises sharply with standard deviation, and the slope of curve $I(V)$ decreases with σ_d for both polarities.

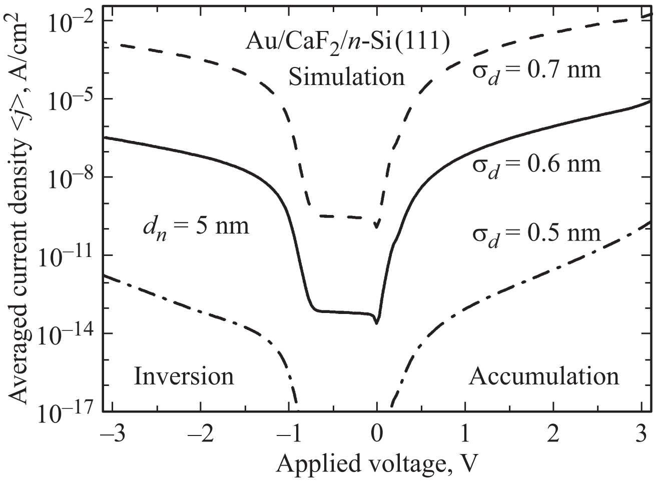

Figure 3. Calculated data demonstrating the influence of film nonuniformity (specified by thickness deviation σ_d) on the current values.

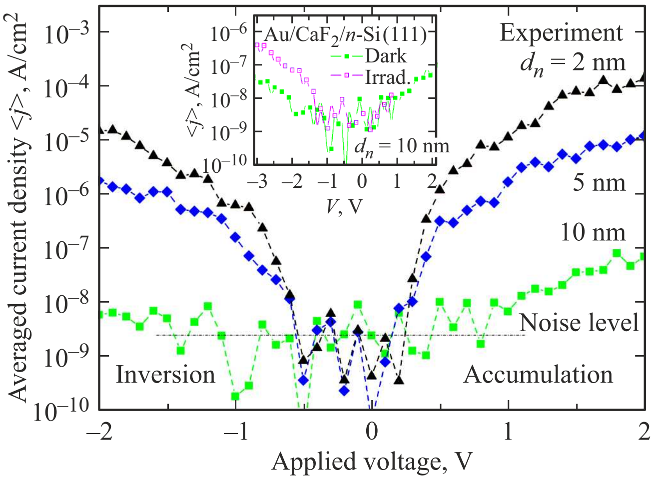

Figure 4. A series of I–V curves recorded for samples with different nominal thicknesses of the fluoride layer in the dark. The photoresponse of one of the samples is shown in the inset. (A color version of the figure is provided in the online version of the paper).

5. Experimental I–V curves

Figure 4 shows the typical measured I–V curves for both polarities. Average current density I/S (S is the area) is plotted on the ordinate axis. The flat-band voltage (with account for the type and level of doping and the barrier heights) is near-zero. The region of negative V values corresponds to depletion or inversion („reverse bias“), while positive V values correspond to accumulation of the MIS structure („direct bias“).

It can be seen that the characteristics are roughly exponential in shape and almost symmetric at different bias polarities. A slight difference in currents measured with increasing and decreasing voltage was observed due to capacitance effects, and the current magnitude decreased somewhat (by a factor of 1.5–2 at the most) in certain cases in repeated measurements (the curves in Fig. 4 represent the regime established after stabilization of currents).

The current decreased markedly with increasing nominal thickness d_n (Fig. 3).

The spread of characteristics from one electrode to the other was roughly half an order of magnitude, which is not much for tunnel structures (especially the ones based on a new material).

The influence of external irradiation on the reverse branch (see the inset of Fig. 4) was noted: the measured current value increased by a factor of 3–5 under irradiation. A red laser served as the radiation source. However, the photoresponse is limited, since photogeneration plays the same role as thermal generation, and the latter is not sufficient to maintain equilibrium in the substrate even in the dark (it is known [17] that the photosensitivity of ultrathin structures, where a current plateau arises at $V < 0$, is higher).

6. Discussion of results

First of all, it is necessary to note that the behavior of Au/CaF$_2$/n-Si(111) samples is in a complete qualitative agreement with the traditional concepts (exponential growth of current with voltage, pronounced dependence on thickness, photoresponse specifics).

An attempt at reproducing the experimental I–V characteristics in calculations was made. Figure 5 presents the curves from Fig. 4 after denoising alongside with the theoretical data. The value of σ_d was the only adjusted parameter. No fitting techniques of the type used occasionally in „tunnel" research (such as altering deliberately the barrier heights, effective masses, or permittivities) were applied.

It turned out that a satisfactory fit is obtained if one sets standard thickness deviation σ_d to 0.21 nm for $d_n = 2$ nm, 0.64 nm for $d_n = 5$ nm, and 1.21 nm for the maximum nominal thickness of 10 nm. These values do not contradict the AFM estimates. That said, σ_d increases at a higher rate than the one specified by a root dependence on d_n; i.e., the growth of new monolayers is less uniform than the growth of preceding ones.

Interpreting the fluctuation data, one needs to take into account that, although calcium fluoride has been studied for a considerable amount of time, CaF$_2$ is still a relatively new material. Therefore, one should not impose on CaF$_2$ the same uniformity requirements as applied to SiO$_2$, HfO$_2$, and similar „industrial" dielectrics (the indicated σ_d values would be very high for such materials [18]). In addition, the nonuniformity itself does not imply that a layer is „bad;" the structural and crystalline quality, reproducibility of parameters, and a high resistance (even if it is lower than the desired one) are more important.

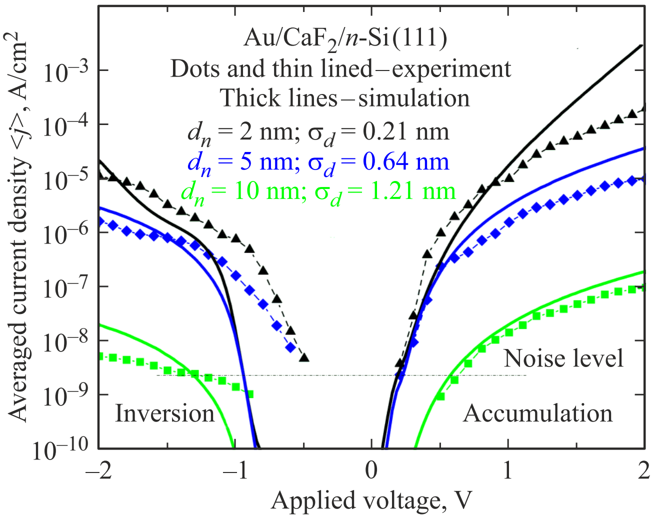

Figure 5. Attempt at reproducing the curves in Fig. 4 (smoothed) in calculations with thickness fluctuations of CaF$_2$ taken into account. The values of σ_d providing a fit are written down.

At the same time, the thickness deviation naturally needs to be reduced in subsequent development of the fabrication technology.

7. Conclusion

Au/CaF$_2$(2–10 nm)/n-Si(111) structures with fluoride layers grown by molecular beam epitaxy were fabricated and examined. The reported results are the first in the 5–10 nm thickness range. A complete qualitative agreement between the current–voltage curves of these structures and traditional concepts regarding the behavior of MIS structures (including the shape of curves and their variation with thickness of the insulator layer and under irradiation) was obtained. The standard deviation of thickness of the grown films estimated by atomic force microscopy and in calculations fell within the range from 0.2 to ~ 1.2 nm. The structures exhibited sufficient reproducibility of their parameters.

It is believed that the studied fluoride films with a nanometer thickness may find application as gate insulators in field-effect transistors (including the ones with a two-dimensional channel). The current stage of research revealed that the epitaxial growth technology is sufficiently mature (the choice of a low (250°C) process temperature was especially significant), which is indicative of the feasibility of fabrication of CaF$_2$ films of a device quality in the mentioned range of nominal thicknesses.

Funding

This study was supported by the Russian Foundation for Basic Research (project ANF_a No. 21-52-14007).

Conflict of interest

The authors declare that they have no conflict of interest.

References

[1] R.F.C. Farrow, P.W. Sullivan, G.M. Williams, G.R. Jones, D.C. Cameron. J. Vac. Sci. Technol., **19**, 415 (1981).
[2] M. Sugiyama, M. Oshima. Microelectronics J., **27**, 361 (1996).
[3] A.A. Velichko, V.A. Ilyushin, A.U. Krupin, V.A. Gavrilenko, N.I. Filimonova, C.C. Kudaev. *Proc. 12th Int. Conf. on Actual Problems of Electronics Instrum. Engineering* (APEIE) (2014) p. 17.
[4] M. Galbiati, M. Scarselli, F. Arciprete, M. De Crescenzi, L. Camilli. J. Phys. D: Appl. Phys., **55**, 095304 (2022).
[5] J. Robertson. Rep. Progr. Phys., **69**, 327 (2006).
[6] W. Hayes. *Crystals with the Fluorite Structure* (Clarendon Press, Oxford, 1974).
[7] M. Tsutsui, M. Watanabe, M. Asada. Jpn. J. Appl. Phys., **38**, Pt 2, No. 8B, L920 (1999).

[8] S. Miyamoto, H. Matsudaira, H. Ishizaka K. Nakazawa, H. Taniuchi, H. Umezawa, M. Tachikia, H. Kawarada. Diamond Relat. Mater., **12**, 399 (2003).

[9] Yu.Yu. Illarionov, A.G. Banshchikov, T. Knobloch, D.K. Polyushkin, S. Wachter, V.V. Fedorov, S.M. Suturin, M. Stöger-Pollach, T. Mueller, M.I. Vexler, N.S. Sokolov, T. Grasser. *Program guide of the 78th Annual IEEE Device Research Conf. (DRC)* (2020) p. 46.

[10] Yu.Yu. Illarionov, T. Knobloch, M. Lanza, D. Akinwande, M.I. Vexler, T. Mueller, M. Lemme, G. Fiori, F. Schwierz, T. Grasser. Nature Commun., **11**, 3385 (2020).

[11] W. Li, J. Zhou, S. Cai, Z. Yu, J. Zhang, N. Fang, T. Li, Y. Wu, T. Chen, X. Xie, H. Ma, K. Yan, N. Dai, X. Wu, H. Zhao, Z. Wang, D. He, L. Pan, Y. Shi, P. Wang, W. Chen, K. Nagashio, X. Duan, X. Wang. Nature Electron., **2**, 563 (2019).

[12] M. Yamamoto, S. Dutta, S. Aikawa, S. Nakaharai, K. Wakabayashi, M.S. Fuhrer, K. Ueno, K. Tsukagoshi. Nano Lett., **15**, 2067 (2015).

[13] S. Watanabe, M. Maeda, T. Sugisaki, K. Tsutsui. Jpn. J. Appl. Phys., **44** (4B), 2637 (2005).

[14] M.I. Vexler, Yu.Yu. Illarionov, S.E. Tyaginov, T. Grasser. Semiconductors, **49**, 259 (2015).

[15] A. Schenk. *Advanced physical models for Silicon device simulations* (Springer, Wien–N.Y., Chap. 5 „Modeling transport across thin dielectric barriers“ (1998) p. 281.

[16] A. Schenk, G. Heiser. J. Appl. Phys., **81**, 7900 (1997).

[17] J. Shewchun, M.A. Green, F.D. King. Solid-State Electron., **17**, 563 (1974).

[18] A. Asenov, S. Kaya, J.H. Davies, S. Saini. Superlatt. Microstruct., **28**, 507 (2000).